

Short Communication

Enhanced Corrosion and Wear Resistance of AZ91 Magnesium Alloy by Fabrication of Galvanized Zn-Al-Mg Coating in Chloride Solution

*Yanqi Wang**, Jun Long, Zhibin Zheng

Institute of New Materials, Guangdong Academy of Sciences, Guangzhou, Guangdong, 510651, China
Guangdong Provincial Key Laboratory of Metal Toughening Technology and Application,
Guangzhou, Guangdong, 510651, China

*E-mail: yale_w@163.com

Received: 2 February 2022 / *Accepted:* 14 March 2022 / *Published:* 5 April 2022

Due to the poor surface properties of the magnesium alloys, a protective Zn-Al-Mg coating with Ni/Cu interlayer was developed on AZ91 magnesium alloy by simple hot-dipping method in this paper. Microstructure of the coated AZ91 magnesium alloy was observed using scanning electron microscope (SEM), optical microscope (OM). The corrosion resistance and wear resistance of the Zn-Al-Mg coating and the magnesium alloy were comparatively investigated by potentiodynamic polarization testing, electrochemical impedance spectroscopy (EIS), friction and wear testing. Results revealed that a dense and uniform Zn-Al-Mg coating, which had a thickness of more than 100 μm , was coated on the magnesium alloy surface. Moreover, the bond between the galvanized Zn-Al-Mg coating and the magnesium alloy substrate was metallurgical, and the hot dipping process had almost no influence on the microstructure of the magnesium alloy. Electrochemical tests in NaCl solution indicated that the corrosion resistance of the coated magnesium alloy had been significantly increased. Further to this, the micro-hardness and wear resistance of the coated magnesium alloy surface were also significantly increased. In addition, the galvanic corrosion between the galvanized Zn-Al-Mg coating and the magnesium alloy was also investigated and discussed.

Keywords: Magnesium alloy; Galvanized coating; Interface; Corrosion; Wear

1. INTRODUCTION

Improving the surface properties of the magnesium alloys, especially the corrosion resistance and wear resistance, is a key to realize the wide application of magnesium alloys in the field of automobile, aviation, electronics and military industries [1, 2]. From the magnesium alloy itself, its corrosion resistance and/or wear resistance can be improved by adding alloy elements (such as Mn, Nd, Gd) or adjusting the microstructure using mechanical deformation [3]; On the other hand, surface

modification technology is another important method to improve the surface properties of magnesium alloys [4-11]. Due to the characteristics of short R&D cycle, simple operation and low cost of the surface modification technology, which arouses the interest of a large number of researchers [4,5,7-9]. The coatings involved in the surface modification of magnesium alloys include organic coatings, inorganic coatings, metal coatings and their composite coatings. It is worth noting that the metal coating not only can provide physical barrier protection to magnesium alloy like other coatings, but also has excellent properties such as electrical conductivity and thermal conductivity, it can meet application scenarios where magnesium alloys have electrical and thermal conductivity requirements, which arouses the interest of the majority of researchers [10, 12-15]. Thermal/cold spraying [9, 12, 16, 17], laser and ion beam [18, 19], electroplating/electroless plating [13, 20-22], thermal diffusion [14], chemical conversion [4, 6, 7], friction stir [15] etc. have been used to construct protective metal coatings on the surface of magnesium alloy. It has been shown that the corrosion resistance and/or wear resistance of magnesium alloys could be significantly improved by coating with the metal coatings.

Compared with the metal coatings such as stainless steel, titanium and titanium alloy, copper, nickel, aluminum and aluminum alloy, the potential difference between zinc coating and magnesium alloy is relatively smaller, which will help to reduce the tendency of galvanic corrosion between magnesium alloy and zinc coating. Moreover, zinc and zinc alloys have excellent corrosion resistance and have been widely used in the corrosion protection of steel [23, 24]. Therefore, zinc coating may be a relatively ideal metal coating for corrosion protection of magnesium alloys. Thermal/cold spraying [12, 16, 17], thermal diffusion [14], and friction stir processing [15] have been used to construct zinc-based coating on the surface of magnesium alloys. However, holes and cracks often appear in the thermal/cold sprayed zinc coating, which can not completely approach the properties of bulk zinc metal. The heat treatment of thermal diffusion zinc coating often requires a long time (100 minutes to more than 10 hours [14, 25]), which means the production efficiency is low. In addition, it is easy to cause temperature rise in the process of coating preparation, which reduce the microstructure and properties of magnesium alloy. Therefore, developing a method, which has high production efficiency and requires short operation time at high temperature, for preparing dense zinc-based coatings on magnesium alloy surface is very necessary.

Keeping this in mind, and inspired by galvanizing process of steel, a galvanized Zn-Al-Mg coating with Ni/Cu interlayer was developed on magnesium alloy to enhance the corrosion resistance and wear resistance of AZ91 magnesium alloy. In this paper, the corrosion and wear behavior of the galvanized Zn-Al-Mg coating on AZ91 magnesium alloy were investigated. The interfacial reaction behavior between Ni/Cu interlayer and zinc bath, Ni/Cu interlayer and the magnesium alloy, and the effect of hot-dipping process on microstructure change of the magnesium alloy were also investigated and discussed.

2. MATERIALS AND METHODS

2.1 Preparation of Ni/Cu interlayer

The as-received AZ91 magnesium alloy, which was cut into plates with 50 mm × 20 mm × 5 mm, was selected as the substrate. The plates surface was polished with 200, 500 and 1000 grit silicon carbide paper in sequence. Then the polished plates were cleaned in alcohol, rinsed in deionized water, and dried with cool air. Then the above-obtained plates were subjected to alkaline degreasing, pickling, activation, zinc leaching, copper and nickel electroplating in sequence, which were described previously [26].

2.2 Preparation of Zn-Al-Mg coating

The samples treated above were rinsed with flowing tap water, and then dipped in a flux bath (95 g/L ZnCl₂ + 150 g/L NH₄Cl) at 60 °C for 60 s. Then the flux coated samples were dried at 120 °C for 100 s in a drying box, they were subsequently galvanized in pure zinc bath at 440 °C for 10 s. Since Al-containing zinc baths are not compatible with chloride based fluxes, the double-dipping process was selected for the preparation of Zn-Al-Mg coating. The sample after taking out from pure zinc bath were immediately dipped in Zn-Al-Mg bath at 410 °C for 15s. Then the coated sample was cooled in air. Note that the Zn-Al-Mg bath had a composition of 5.32 wt.% Al, 2.40 wt.% Mg, and balance Zn.

2.3 Coating characterization

Scanning electron microscope (SEM) equipped with EDS (GeminiSEM300) was used to characterize the cross-sectional morphology and elemental compositions of the galvanized Zn-Al-Mg coating. ZH-U-S hardness tester ($f = 10$ g, $t = 10$ s) was used to measure the microhardness distribution from the surface of galvanized Zn-Al-Mg layer to the interior of magnesium matrix. Wear tests were carried out with the parameters: load $F = 20$ N, friction stroke length $L = 4.5$ mm, friction pair diameter $D = 4$ mm (440 stainless steel), and friction frequency $f = 4$ Hz, time $t = 30$ min. After the friction and wear test, wear traces were observed by on-line optical profilometer (DEKTAK XT).

The corrosion behaviour of the AZ91 magnesium alloy and the galvanized Zn-Al-Mg coating was estimated by electrochemical measurements using an electrochemical workstation (Gamry Interface 1000E). The samples were mounted with an exposed area $S = 1$ cm². A three electrode cell with specimen as the working electrode, platinum as the counter electrode, and saturated calomel electrode as the reference electrode were performed. EIS spectra were collected with frequency range 10^5 Hz – 10^{-2} Hz and an amplitude 10 mV at open circuit potential. Potentiodynamic polarization curves were obtained in the corrosive solution at a scanning rate of 0.1 mV/s.

3. RESULTS

3.1 Cross-sectional observation of the Zn-Al-Mg coating

The cross-sectional SEM backscattered images of the Ni/Cu layer and the galvanized Zn-Al-Mg coating is present in Fig. 1. The thickness of the Ni/Cu layer is about 25 μm (see the bright layer Fig. 1a). Fig. 1b is a partial enlarged view of Fig. 1a, the lines scanning of the Ni/Cu coating reveals that, before hot-dip galvanizing, the Ni/Cu coating is composed of a Ni layer with about 6 μm and a Cu layer with about 19 μm .

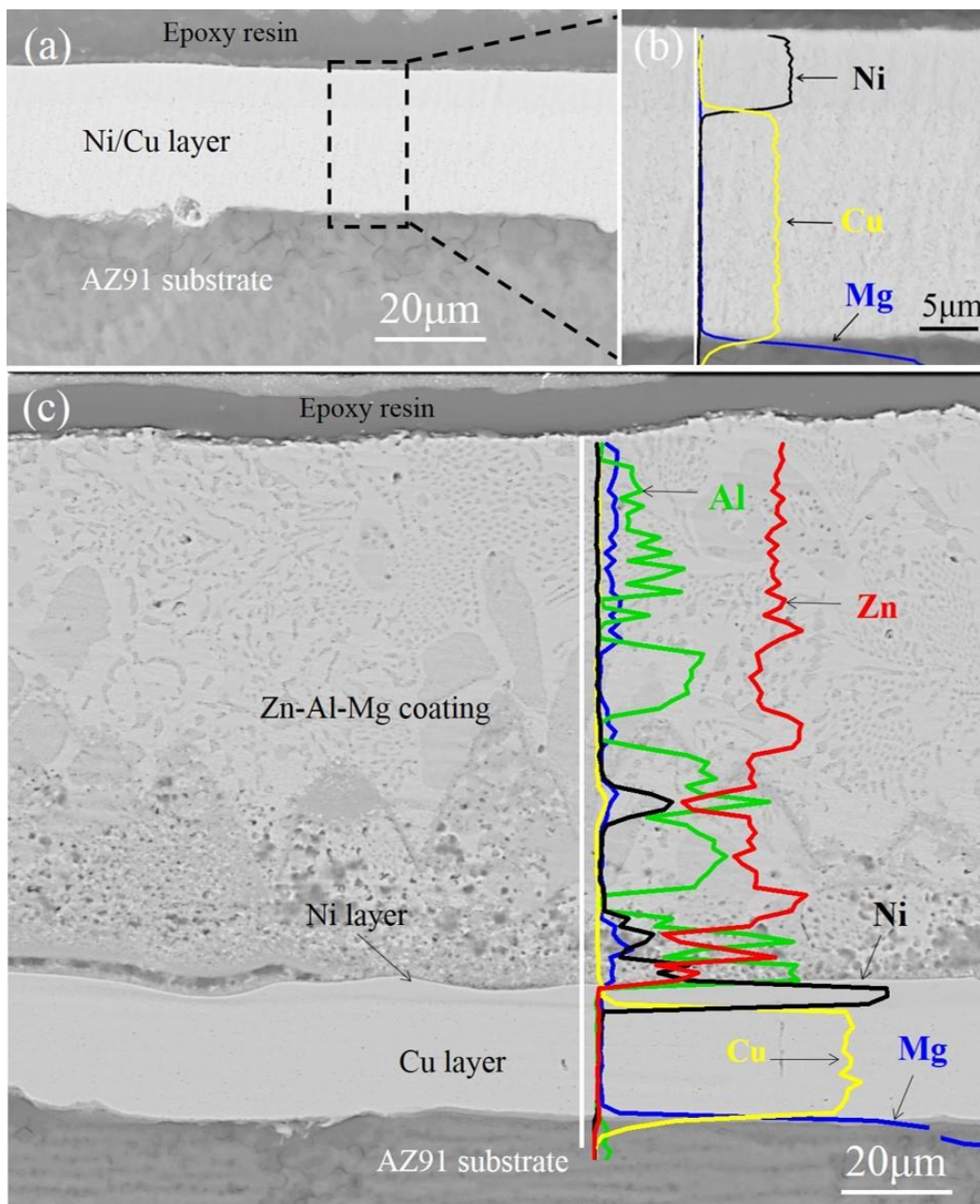


Figure 1. Cross-sectional SEM backscattered images for: a) the Ni/Cu layer and b) the galvanized Zn-Al-Mg coating.

In Fig. 1c, one can observe that the resultant galvanized Zn-Al-Mg coating mainly includes two layers, that is a Zn-Al-Mg out layer with about 100 μm and Cu inner layer with 19 μm . However, the line scanning in Fig. 1c indicate that a layer of Ni, which has a thickness from 1 μm to 3 μm , still exists between the Zn-Al-Mg layer and Cu layer, indicative of a layer of Ni with a thickness 3~5 μm was dissolved during hot-dip galvanizing process. Moreover, the line scanning of Ni also reveals that the Ni layer was dissolved into the Zn-Al-Mg layer. The result of line scanning for Al shows that Al content near Ni layer is higher than that in other areas, implying Al enrichment occurs near the Ni layer.

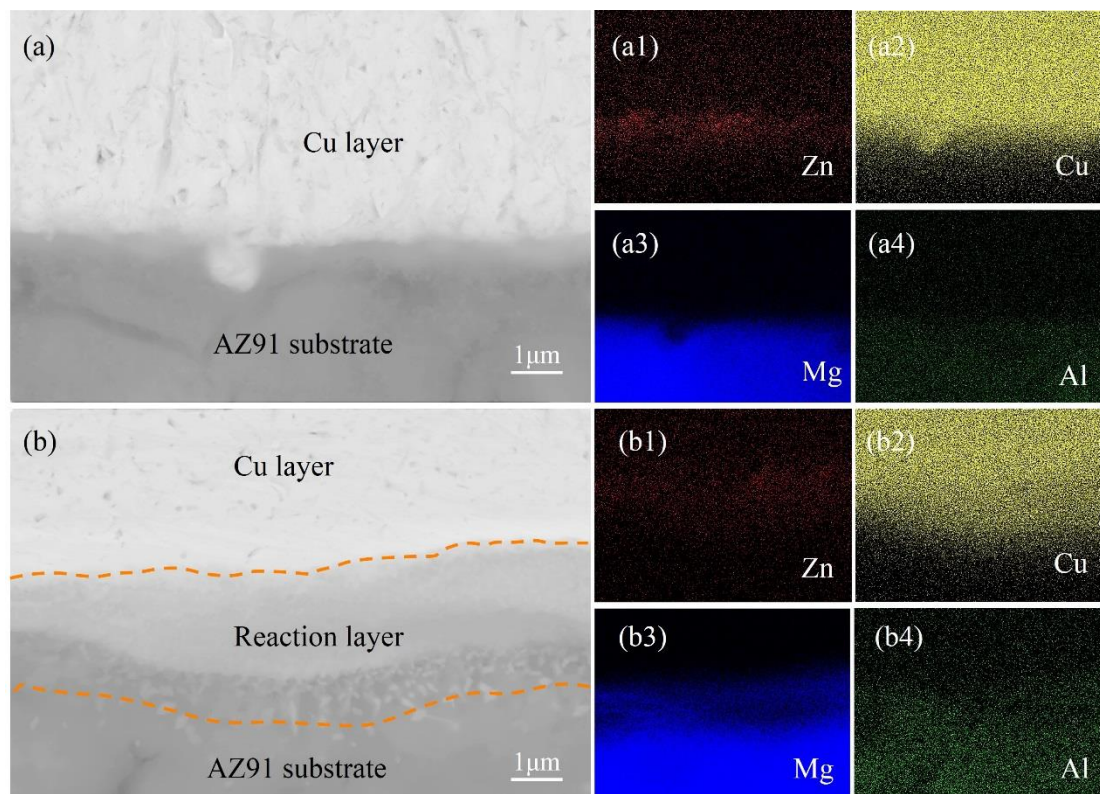


Figure 2. Interface morphology between AZ91 magnesium alloy substrate and Ni/Cu interlayer: a) before hot-dip galvanizing and b) after hot-dip galvanizing; a1-a4: map scanning of Zn, Cu, Mg and Al for Fig. 2a; b1-b4: map scanning of Zn, Cu, Mg and Al for Fig. 2b.

The interface morphology between the Ni/Cu interlayer and the magnesium alloy was further studied. Fig. 2 shows interface layers between AZ91 magnesium alloy substrate and Ni/Cu interlayer before and after hot-dip galvanizing. when compared with the interface morphology in Figs. 3a and 3b, a remarkable change can be observed at the interface between Cu layer and the magnesium alloy after hot-dip galvanizing process. In Fig. 2a, the Ni/Cu layer and the magnesium alloy are basically in direct contact with each other without a reaction layer. The map scanning in Figs. 3a1-a4 shows that a small amount of residual zinc layer exists between the Ni/Cu layer and the magnesium alloy. The residual zinc layer should come from the zinc leaching before Cu electroplating. In Fig. 2b, it can be seen that the formation of an obvious reaction/diffusion layer appears between the Ni/Cu interlayer and the magnesium alloy, indicative of a metallurgical bond is formed between the Ni/Cu interlayer and AZ91

magnesium alloy. Moreover, elemental maps result in Figs. 3b1-b4 reveals that the reaction/diffusion layer is mainly composed of Cu, Mg and Zn.

Fig. 3 shows the microstructures of the AZ91 magnesium alloy before and after hot-dip galvanizing. In Fig. 3, one can observe that the size, shape and distribution of the grain in the AZ91 magnesium alloy had basically not changed when compared with the microstructures of the AZ91 magnesium alloy obtained before and after hot-dip galvanizing. The result reveals that, the effect of the hot-dipping process on the microstructure and physical properties of magnesium alloy was very limited.

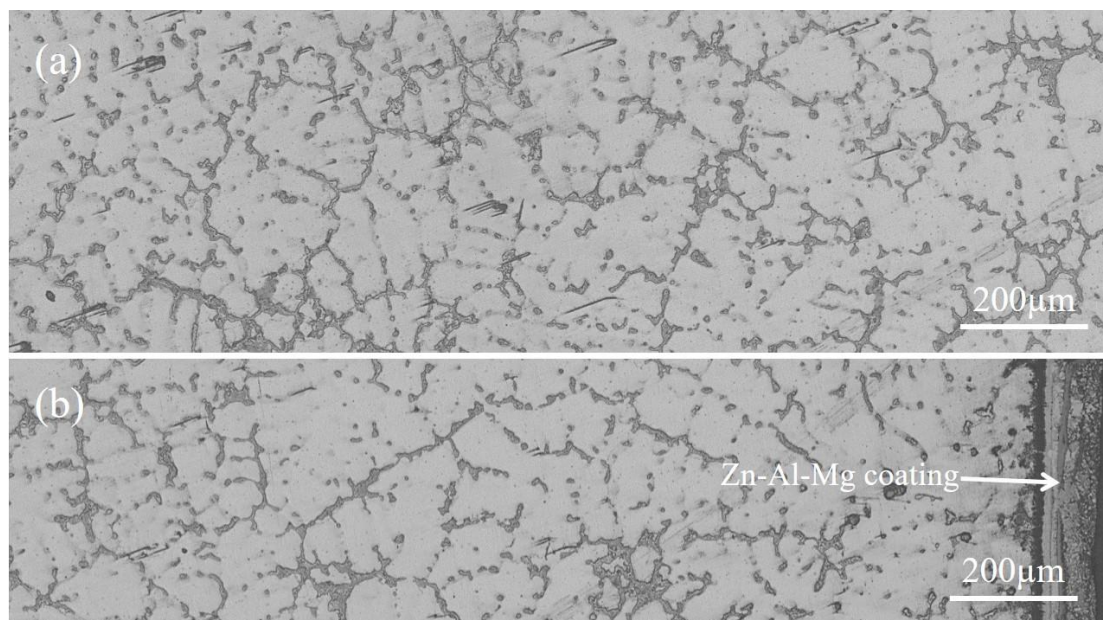


Figure 3. OM images of AZ91 magnesium alloy: a) as-received, b) after hot-dip galvanized process.

3.2 Corrosion behaviour in NaCl solution

3.2.1 Evaluation of electrochemical corrosion behaviour

The corrosion resistance of the magnesium alloy and the galvanized Zn-Al-Mg coating were evaluated by potentiodynamic polarization curve, and the results are displayed in Fig. 4. In Fig. 4, one can observe that the experimental anodic Tafel region of the two polarization curves is not well defined. Consequently, the corrosion current density (i_{corr}) and cathode tafel slope (b_c) were determined by extrapolating the cathodic Tafel region illustrated in Fig. 4 [27]. The fitting parameters are list in Table 1. As seen in Table 1, the corrosion potential (E_{corr}) of the AZ91 magnesium alloy and the Zn-Al-Mg coating are -1.56 V (vs. SCE) and -1.05 V (vs. SCE), respectively. The corrosion current densities (i_{corr}) of the magnesium alloy and the Zn-Al-Mg coating are $79.35 \mu\text{A}/\text{cm}^2$ and $0.42 \mu\text{A}/\text{cm}^2$, respectively. It suggests that the corrosion resistance of the magnesium alloy could be significantly improved by coating with the galvanized Zn-Al-Mg coating.

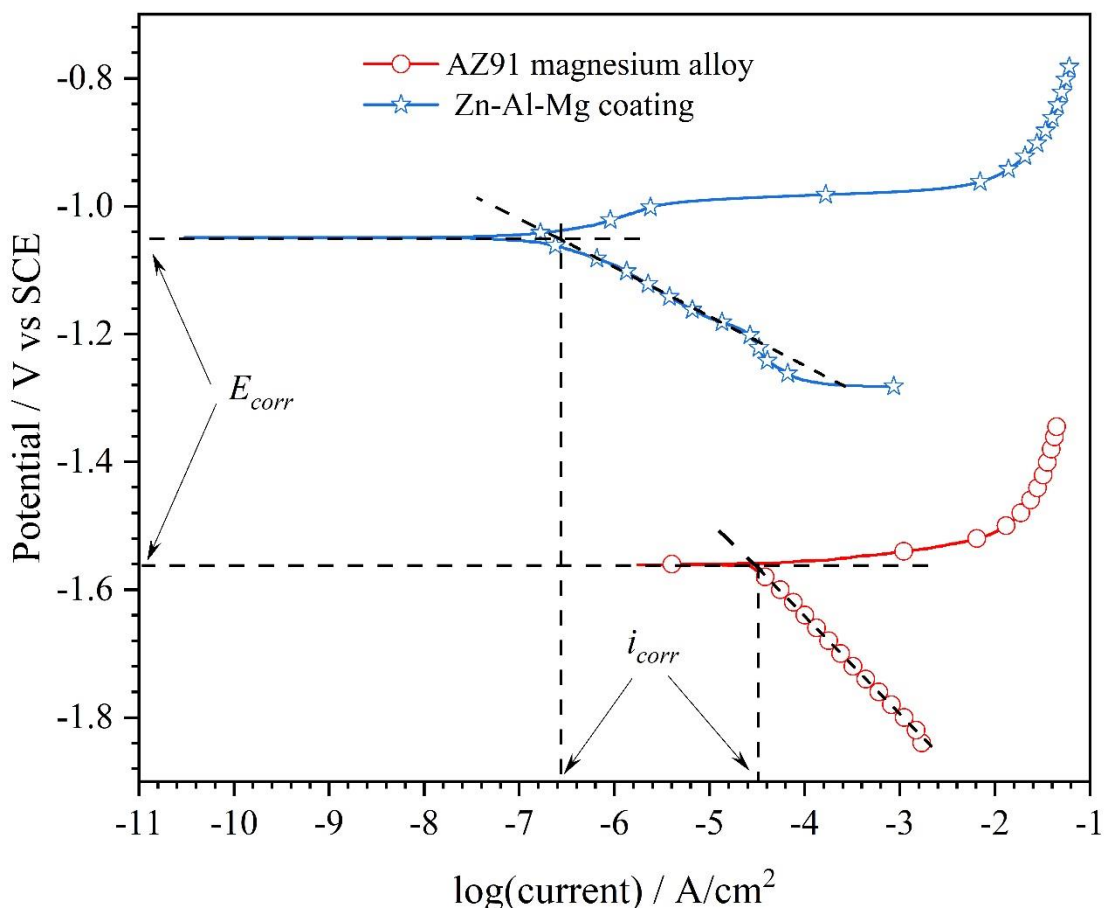


Figure 4. Potentiodynamic polarization curves of the magnesium alloy and the galvanized Zn-Al-Mg coating.

Table 1. Fitting parameters obtained in Figure 5.

sample	E_{corr} / V vs SCE	i_{corr} / $\mu\text{A}/\text{cm}^2$	b_a / mV/decade	b_c / mV/decade
AZ91	-1.56	29.61	-	-152.9
Zn-Al-Mg coating	-1.05	0.42	-	-91.8

Fig. 5 displays the EIS spectra of the magnesium alloy and the galvanized Zn-Al-Mg coating. When observe the Nyquist diagram for the magnesium alloy, it can be seen that the Nyquist diagram presents two loops, which is well-defined. In detail, a capacitance loop is occurred at the high frequencies, and an inductive loop is occurred at the low frequencies. At high frequencies, the capacitance loop could describe the charge transfer process of Mg/Mg^{2+} at the double layer. The diameter of the capacitance loop can be used to evaluate the charge transfer resistance of the magnesium alloy electrode [27]. The inductive loop represents the desorption of the corrosion products and the reaction of Mg^+ with H_2O [28]. The Nyquist plot of the galvanized Zn-Al-Mg coating presents two distinct capacitive loops. The first capacitive loop which appears at high frequency is related to penetration of

electrolyte; the second capacitive loop which appears at low frequency is related to the charge transfer, and the double layer behaviour [23].

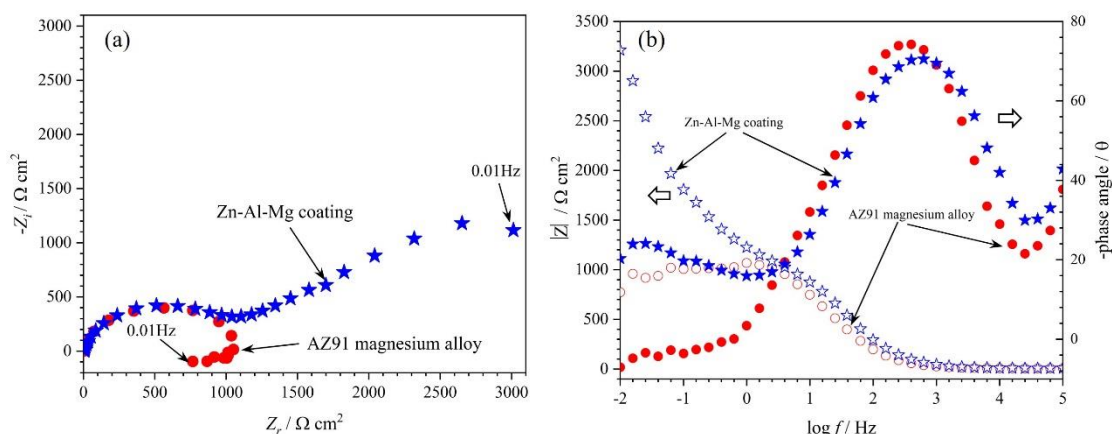


Figure 5. EIS spectra of the magnesium alloy and the Zn-Al-Mg coating.

The equivalent circuit used to fit the EIS spectra is presented in Fig. 6. Table 2 lists the calculated values. The meaning of the symbol is illustrated in Fig. 6. *CPE* is usually used instead of a pure capacitance. And the impedance of *CPE* is calculated as follows: $Z_{CPE} = (Y_0)^{-1}(j\omega)^{-n}$, where Y_0 , j , ω and n are defined in Fig. 5 [23]. Generally, the reciprocal of R_p (polarization resistance) is proportional to the corrosion resistance of the samples [27]. Based on the equivalent circuit model in Fig. 6a, the value of $1/R_p$ could be calculated by the equation:

$$R_p = \frac{R_1 * R_2}{R_1 + R_2} \quad (1)$$

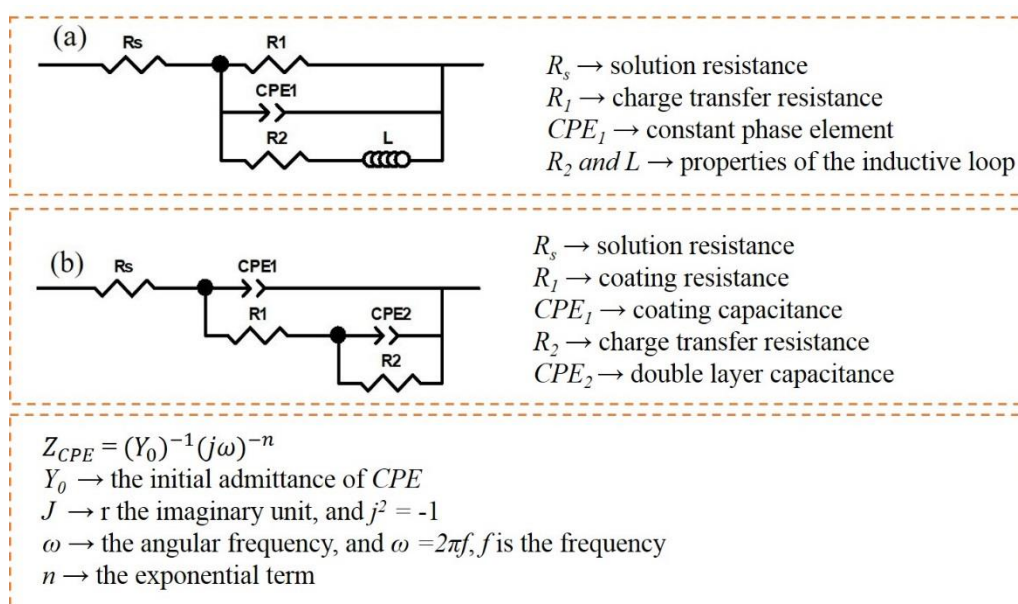


Figure 6. Equivalent circuit for EIS spectra fitting in this paper.

Table 2. Fitting parameters of EIS data in Figure 6. The unit for resistance is $\Omega \text{ cm}^2$, Y_0 is $10^{-6} \Omega^{-1} \text{ cm}^{-2} \text{ s}^{-n}$, L is H cm^{-2} .

Sample	R_s	R_1	Y_{01}	n_1	R_2	Y_{02}	n_2	L	R_p
AZ91	5.65	4083	17.41	0.88	1030	-	-	26210	823
Zn-Al-Mg coating	5.48	1042	14.17	0.84	4859	1234	0.56	-	5901

Table 2 suggests that $1/R_p$ value of the galvanized Zn-Al-Mg coating is obviously much smaller than that of the AZ91 magnesium alloy. It indicates that the corrosion resistance of the galvanized Zn-Al-Mg coating much higher than that of the AZ91 magnesium alloy. The result is in good agreement with that obtained in Fig. 4. However, the corrosion potential of the Zn-Al-Mg coating is higher than that of the magnesium alloy (see Table 1), then it is easy to form galvanic corrosion between the magnesium alloy and the Zn-Al-Mg layer, which may accelerate the corrosion of the magnesium alloy. In conclusion, ensuring that the galvanized Zn-Al-Mg coating has a certain thickness and its integrity should be very important to the improvement of corrosion resistance of magnesium and its alloys.

3.2.3 Cut-edge corrosion behaviour in NaCl solution

The galvanic corrosion behaviour between the galvanized Zn-Al-Mg coating and the AZ91 magnesium alloy was investigated in 3.5% NaCl solution. The cut-edge corrosion morphology of the Zn-Al-Mg coated AZ91 magnesium alloy after 5h immersion is illustrated in Fig. 7. It can be observed that the whole surface of the magnesium alloy was corroded, and obvious corrosion products were formed on the surface of the magnesium alloy. Notably, more corrosion products are seen in the area near the Zn-Al-Mg coating than that in other areas on the magnesium alloy. This phenomenon indicates that galvanic corrosion occurs between the magnesium alloy and the coating in NaCl solution, by which leading to accelerated corrosion of the magnesium alloy substrate near the coating, thus forming more corrosion products in the areas near the Zn-Al-Mg coating. However, in Fig. 7a, significant corrosion pits can be seen on the magnesium alloy surface far away from the coating, which indicates that, when compared with the harmfulness of pitting corrosion on the AZ91 magnesium alloy, galvanic corrosion between the magnesium alloy and the Zn-Al-Mg coating is acceptable. The elemental maps in Figs. 8c-h reveal that the corrosion products mainly composed of Mg and O elements, and some corrosion products containing Mg may migrate to the surface of the Zn-Al-Mg coating.

The corrosion morphology of the coated AZ91 magnesium alloy after 36h immersion is presented in Fig. 8. In Fig. 8a, it can be seen that severe corrosion occurred on the whole magnesium alloy surface, except for the Zn-Al-Mg coating and some areas close to the coating. It can be seen in Fig. 8a, the corrosion products formed on the surface of the magnesium alloy are loose and porous. Fig. 8b presents the corrosion morphology of the Zn-Al-Mg coating and some areas on the magnesium alloy near the coating. One can see that a layer of corrosion products, whose morphology is different from that in other areas, was formed on the surface of the magnesium alloy and the Zn-Al-Mg coating. It suggests

that some areas on the magnesium alloy adjacent to the Zn-Al-Mg coating was even protected with limited corrosion.

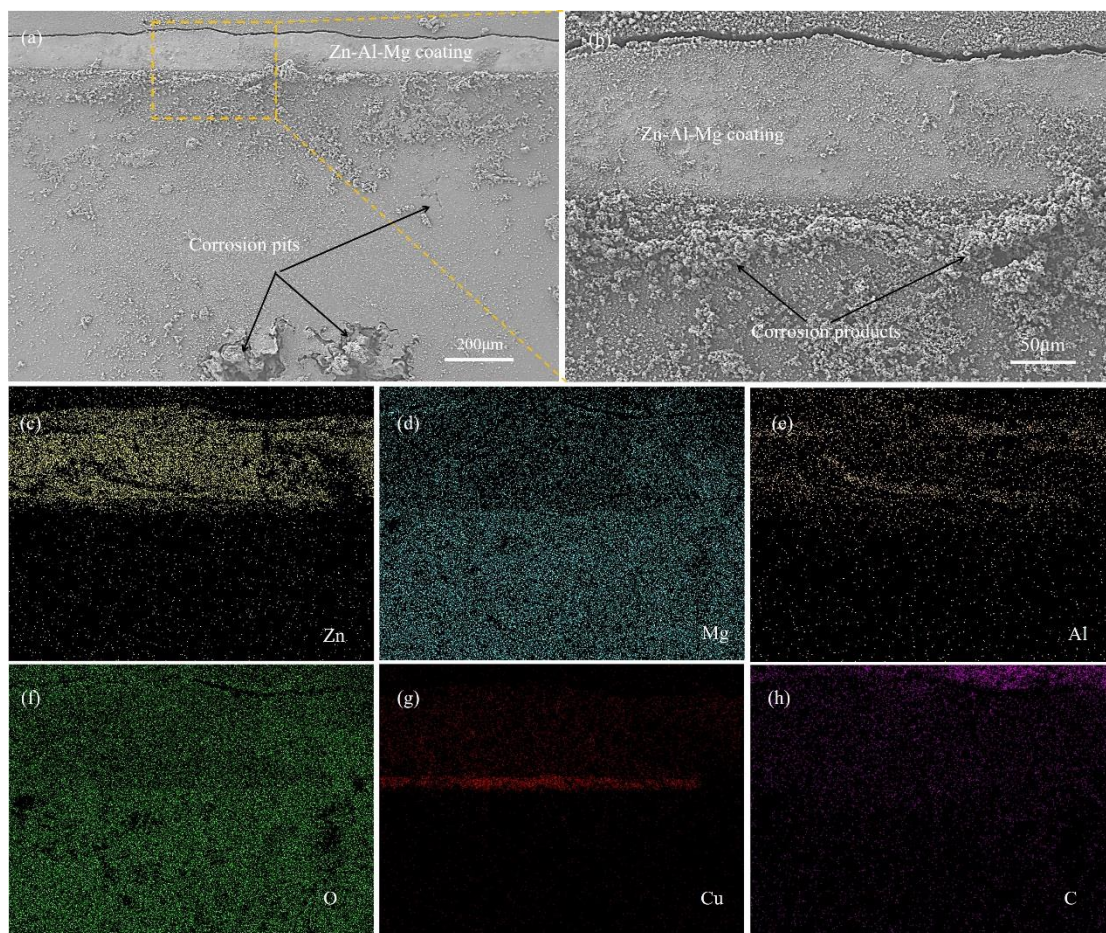


Figure 7. Cross-sectional morphology of Zn-Al-Mg coated AZ91 magnesium alloy in NaCl solution after 5h immersion. Elemental maps for Fig. 7b are shown in Fig. 8c-h.

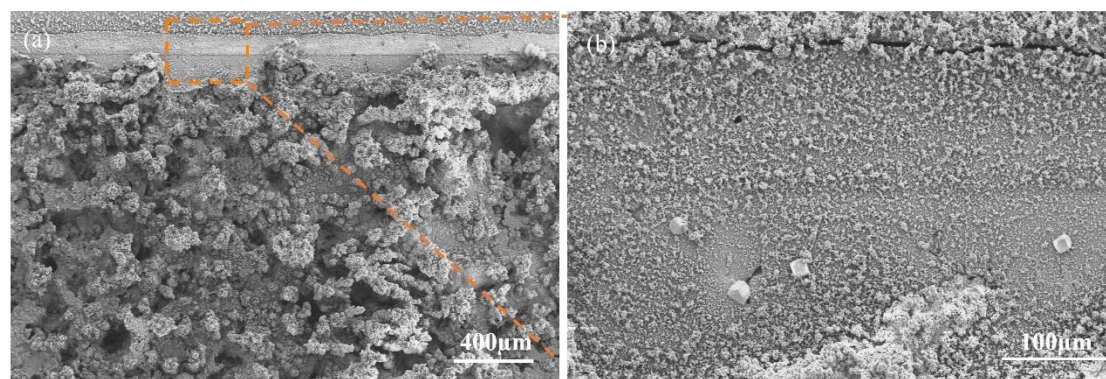


Figure 8. Cross-sectional morphology of Zn-Al-Mg coated AZ91 magnesium alloy in NaCl solution after 36h immersion.

3.3 Friction and wear behaviour

Fig. 9a shows the micro-hardness profile crossing the Zn-Al-Mg coating. Micro-hardness of the Zn-Al-Mg layer, Ni/Cu interlayer and the AZ91 magnesium alloy have been represented. The micro-hardness profile suggests that the average micro-hardness of the Zn-Al-Mg coating and the AZ91 magnesium alloy substrate are 282 HV and 78 HV, respectively. The micro-hardness of the Zn-Al-Mg coating is almost four times than that of the magnesium alloy. As for the Ni/Cu interlayer, it has a micro-hardness about 120 HV. Apparently, the micro-hardness of the Ni/Cu interlayer is also much higher than that of the magnesium alloy. The increase of the surface hardness will be helpful for the improvement of the wear resistance of the magnesium alloy [14].

Fig. 9b shows cross-sectional profiles of wear tracks for the AZ91 magnesium alloy and the galvanized Zn-Al-Mg coating. The AZ91 magnesium alloy presents a wear depth about 131 μm , and a wear width about 1356 μm . However, the Zn-Al-Mg coating exhibits a wear depth about 69 μm , and a wear width about 1065 μm . It is suggested that the wear resistance of the Zn-Al-Mg coating is significantly higher than that of the AZ91 magnesium alloy. Then the wear resistance of the AZ91 magnesium alloy can be significantly enhanced by coating with the galvanized Zn-Al-Mg coating. In a word, the micro-hardness and wear tests indicate that, the hot-dip galvanizing of the magnesium alloy would be an effective way to improve the wear resistance of the magnesium alloy surface.

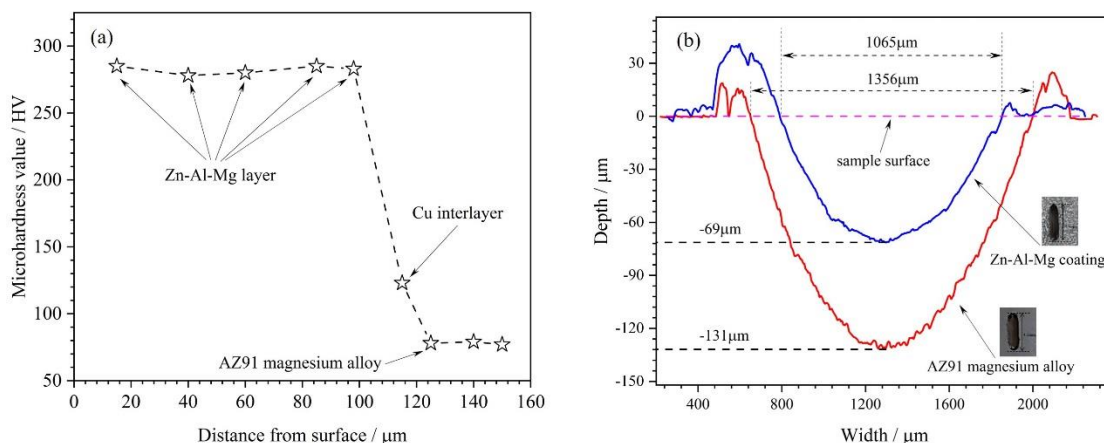


Figure 10. a) Micro-hardness distribution of the Zn-Al-Mg coating on the surface of the AZ91 magnesium alloy, and b) Cross-section profiles of wear tracks for the AZ91 magnesium alloy and the galvanized Zn-Al-Mg coating.

4. DISCUSSION

4.1 Formation of the Zn-Al-Mg coating with Ni/Cu interlayer

According to the Mg-Zn binary phase diagram [29], the melting point of the Mg-Zn intermetallic compounds are lower than that of the zinc bath (about 440°C). When the magnesium alloy immersed in the zinc bath, a high melting point protective layer at the interface between the magnesium alloy and the

zinc bath cannot be formed, resulting in quick dissolution of magnesium alloy in zinc bath. Therefore, in this paper, a high melting point Ni interlayer was pre-plated on the surface of the AZ91 magnesium alloy substrate (Fig. 1a). as seen in Fig. 11a and b, the Ni/Cu interlayer on the magnesium alloy surface has two main functions: 1) avoid severe dissolution of the magnesium alloy in acid pickling and fluxing solution, 2) prevent the magnesium alloy from directly contacting the zinc bath, by which avoiding rapid dissolution of the magnesium alloy in zinc bath. This paper mainly focuses on the interfacial reaction between nickel layer and the zinc bath, as well as the interfacial reaction between copper layer and the magnesium alloy.

Cross-sectional observation of the Zn-Al-Mg coating in Figs. 2 and 3 indicates that, a reaction/diffusion layer was formed at the interface between Zn-Al-Mg layer and Ni/Cu interlayer, and a reaction/diffusion layer was also formed at the interface between Ni/Cu interlayer and the AZ91 magnesium alloy. As seen in Fig. 11c, when Ni/Cu layer coated samples were immersed in pure zinc bath, Ni layer began to dissolve, accompanied by the formation of Ni-Zn intermetallic compounds [30, 31](such as δ -NiZn₈, γ -Ni₂Zn₅ and γ_1 -NiZn₃). The formation of the Ni-Zn intermetallic compounds would act as a protective layer to inhibit Ni layer from further dissolution. As the samples were dipped in the Zn-Al-Mg bath, Zn, Al, Mg atoms diffused toward the Ni layer. Since the atomic radius of Al and Mg is smaller than that of Zn, Al and Mg would diffuse faster than Zn, resulting in the enrichment of Al and Mg near the nickel layer (see the line scanning in Fig. 1c). As shown in Fig. 1c (the gray areas near the Ni layer), the formation of Al-Ni intermetallic compounds [32](such as Ni₃Al, NiAl, Ni₂Al₃ and NiAl₃) and Mg-Ni intermetallic compounds [33](such as NiMg₂ and NiMg₂) would occur at the interface between Ni layer and Zn-Al-Mg bath.

As for the reaction/diffusion layer between the Ni/Cu interlayer and the magnesium alloy, elemental maps in Figs. 3b1-b4 reveal that, it mainly contains Mg, Cu and Zn elements. During hot-dip galvanizing, the residual Zn layer (Fig. 1a) which derived from zinc leaching may be melt and reacted with the Cu interlayer and the magnesium alloy. The melt zinc may promote the mutual diffusion between Mg atoms and Cu atoms, then form the obvious reaction/diffusion layer (Fig. 1b). According to Mg-Cu and Mg-Zn binary phase diagram [33-35], the reaction/diffusion layer may be composed of Mg-Cu, Mg-Zn, Cu-Zn, Mg-Zn-Cu intermetallic compounds (Fig. 11c). The formation of the reaction/diffusion layer is helpful to improve the bonding strength between the galvanized Zn-Al-Mg coating and the magnesium alloy substrate.

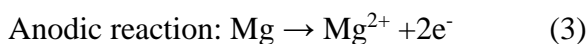
This study shows that galvanized Zn-Al-Mg coating with high corrosion resistance could be successfully constructed on the surface of magnesium alloy by using Ni/Cu as interlayer. However, further research is needed to preform to understand the dissolution behaviour of Ni layer in zinc bath. Since the purpose of pre-copper electroplating is to obtain a uniform and dense nickel coating on Mg surface, then the pre-copper layer could be thinner in practical production and application.

4.2 Corrosion behavior of the coated AZ91 magnesium alloy

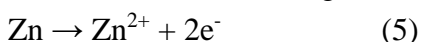
Both results obtained from the potentiodynamic polarization curves in Fig. 4 and the EIS spectra in Fig. 5 show that the corrosion resistance of the AZ91 magnesium alloy could be effectively improved

through hot-dip galvanizing. The magnesium alloy could be separated from the corrosive ion (such as Cl⁻) by coating with Zn-Al-Mg layer, and the galvanized Zn-Al-Mg coating shows better corrosion resistance than the magnesium alloy in the NaCl solution, then the surface property of the magnesium alloy could enhance with Zn-Al-Mg coating. Since the service life of the galvanized Zn-Al-Mg coating is proportional to its thickness, it is necessary to obtain a certain thickness of the Zn-Al-Mg coating on the magnesium alloy surface.

The cut-edge corrosion behaviour for the Zn-Al-Mg alloy coated magnesium alloy in NaCl solution reveals that, galvanic corrosion between Zn-Al-Mg coating and the magnesium alloy occurred in early stage, by which increased the corrosion of some areas of the magnesium alloy matrix adjacent to the Zn-Al-Mg coating. However, when compared with the obvious corrosion pits formed on the magnesium alloy, the corrosion degree derived from the galvanic corrosion between the magnesium alloy and the Zn-Al-Mg coating was acceptable. Moreover, after long-time immersion (36h), it is interesting that some areas on the magnesium alloy, which adjacent to the Zn-Al-Mg coating, were even protected without significant corrosion. When the coated magnesium alloy immersed in NaCl solution, the magnesium alloy would act as anode, the Zn-Al-Mg coating and Ni/Cu interlayer would act as cathode:



Since Zn and Al are amphoteric metal, as OH⁻ accumulation on cathode areas resulting in pH increase, Zn and Al in Zn-Al-Mg coating may be dissolved:



The dissolution of Zn and Al in the Zn-Al-Mg coating, on one hand, may show inhibition effect on reaction (3), reducing the dissolution of the magnesium alloy; on the other hand, Zn²⁺ and Al³⁺ may participate in the formation of the dense corrosion products containing Zn, Al and Mg [36], which may migrate to the magnesium alloy surface. Then one can observe that, the magnesium alloy adjacent to the Zn-Al-Mg coating was even protected with limited corrosion. Therefore, the magnesium alloy with a certain coating break or crack may show self-healing property, which is worthy of further study.

4. CONCLUSIONS

A protective Zn-Al-Mg coating with Ni/Cu interlayer, which had a thickness of more than 100 μm, was developed on AZ91 magnesium alloy by a simple hot-dipping method in this paper. The following conclusions can be drawn:

1. The bond between the galvanized Zn-Al-Mg coating and the magnesium alloy substrate was metallurgical. During hot-dip galvanizing, the Ni/Cu interlayer reacted with the magnesium alloy, which leads to metallurgical bonding between magnesium alloy and Ni/Cu interlayer.
2. Optical microscope observation suggests that, the double-dipping process had almost no influence on the microstructure of the AZ91 magnesium alloy. The structure and properties of the magnesium alloy can still remain unchanged after the double-dipping process.

3. The corrosion and wear resistance of the AZ91 magnesium alloy surface were significantly improved by coated with the galvanized Zn-Al-Mg coating. In addition, the galvanic corrosion between the AZ91 magnesium alloy and the Zn-Al-Mg coating can be ignored when compared with the corrosion degree of the bulk AZ91 magnesium alloy itself. Interestingly, it was even observed that the magnesium alloy substrate adjacent to the Zn-Al-Mg coating was even protected with limited corrosion.

ACKNOWLEDGEMENTS

This work was supported by GDAS' Special Project of Science and Technology Development [2020GDASYL-20200103135].

References

1. Y. Yang, X. Xiong, J. Chen, X. Peng, D. Chen, F. Pan, *J. Magnesium Alloys*, 9 (2021) 705-747.
2. J. Song, J. She, D. Chen, F. Pan, *J. Magnesium Alloys*, 8 (2020) 1-41.
3. M. Esmaily, J.E. Svensson, S. Fajardo, N. Birbilis, G.S. Frankel, S. Virtanen, R. Arrabal, S. Thomas, L.G. Johansson, *Prog. Mater. Sci.*, 89 (2017) 92-193.
4. H. Zhu, X. Li, X. Guan, Z. Shao, *Met. Mater. Int.*, 27 (2021) 3975-3982.
5. Q. Liang, *Int. J. Electrochem. Sci.*, (2021) 210647.
6. J. Qi, Z. Ye, N. Gong, X. Qu, D. Mercier, J. Światowska, P. Skeldon, P. Marcus, *Corros. Sci.*, 186 (2021) 109459.
7. W. Zai, X. Zhang, Y. Su, H.C. Man, G. Li, J. Lian, *Surf. Coat. Technol.*, 397 (2020) 125919.
8. K. Cao, *Int. J. Electrochem. Sci.*, (2021) 210328.
9. H.-L. Yao, Z.-H. Yi, C. Yao, M.-X. Zhang, H.-T. Wang, S.-B. Li, X.-B. Bai, Q.-Y. Chen, G.-C. Ji, *Ceram. Int.*, 46 (2020) 7687-7693.
10. X. Guan, H. Zhu, J. Shi, S. Wei, Z. Shao, X. Shen, *Surf. Eng.*, 35 (2019) 906-912.
11. H. Yang, *Int. J. Electrochem. Sci.*, (2020) 12203-12219.
12. K. Wang, S. Wang, T. Xiong, D. Wen, G. Wang, W. Liu, H. Du, *Surf. Coat. Technol.*, 387 (2020) 125549.
13. S. Taşci, R.C. Özden, M. Anik, *Met. Mater. Int.*, 25 (2019) 313-323.
14. H. Wang, B. Yu, W. Wang, G. Ren, W. Liang, J. Zhang, *J. Alloys Compd.*, 582 (2014) 457-460.
15. H. Yuan, L. Zhang, L. Wu, S. Zhu, Y. Sun, S. Guan, *Mater. Lett.*, 289 (2021) 129389.
16. C. Xie, H. Li, X. Zhou, C. Sun, *Surf. Coat. Technol.*, 374 (2019) 797-806.
17. Y. Bai, Z.H. Wang, X.B. Li, G.S. Huang, C.X. Li, Y. Li, *J. Alloys Compd.*, 719 (2017) 194-202.
18. S. Jana, M. Olszta, D. Edwards, M. Engelhard, A. Samanta, H. Ding, P. Murkute, O.B. Isgor, A. Rohatgi, *Corros. Sci.*, 191 (2021) 109707.
19. F. Iranshahi, M.B. Nasiri, F.G. Warchomicka, C. Sommitsch, *J. Magnesium Alloys*, 8 (2020) 1314-1327.
20. W. Shang, X. Zhan, Y. Wen, Y. Li, Z. Zhang, F. Wu, C. Wang, *Chem. Eng. Sci.*, 207 (2019) 1299-1308.
21. C. Hu, M. Xu, J. Zhang, B. Hu, G. Yu, *J. Alloys Compd.*, 770 (2019) 48-57.
22. Y.-r. ZHOU, S. ZHANG, L.-l. NIE, Z.-j. ZHU, J.-q. ZHANG, F.-h. CAO, J.-x. ZHANG, *Trans. Nonferrous Met. Soc. China*, 26 (2016) 2976-2987.
23. S. Peng, S.-K. Xie, F. Xiao, J.-T. Lu, *Corros. Sci.*, 163 (2020) 108237.
24. D. Persson, D. Thierry, O. Karlsson, *Corros. Sci.*, 126 (2017) 152-165.
25. F. Liu, W. Liang, X. Li, X. Zhao, Y. Zhang, H. Wang, *J. Alloys Compd.*, 461 (2008) 399-403.
26. J. Tang, K. Azumi, *Electrochim. Acta*, 56 (2011) 8776-8782.
27. Y. Ma, H. Xiong, B. Chen, *Corros. Sci.*, 191 (2021) 109759.

28. T. Zhang, G. Meng, Y. Shao, Z. Cui, F. Wang, *Corros. Sci.*, 53 (2011) 2934-2942.
29. T.A. Vida, C. Brito, T.S. Lima, J.E. Spinelli, N. Cheung, A. Garcia, *Current applied physics*, 19 (2019) 582-598.
30. Y. Tan, R. Zhuang, G. Yang, X. Tao, H. Chen, Y. Ouyang, Y. Du, *J. Alloys Compd.*, 881 (2021) 160581.
31. G. Kong, J. Lu, Q. Xu, *Journal of Wuhan University of Technology-Mater. Sci. Ed.*, 23 (2008) 712-716.
32. K. Morsi, *Materials Science and Engineering: A*, 299 (2001) 1-15.
33. J. Miettinen, *Calphad*, 32 (2008) 389-398.
34. Y. Grosu, A. Zaki, A. Faik, *Appl. Surf. Sci.*, 475 (2019) 748-753.
35. S. Zhou, Y. Wang, F.G. Shi, F. Sommer, L.-Q. Chen, Z.-K. Liu, R.E. Napolitano, *J. Phase Equilib. Diffus.*, 28 (2007) 158-166.
36. T. Ishikawa, M. Ueda, K. Kandori, T. Nakayama, *Corros. Sci.*, 49 (2007) 2547-2556

© 2022 The Authors. Published by ESG (www.electrochemsci.org). This article is an open access article distributed under the terms and conditions of the Creative Commons Attribution license (<http://creativecommons.org/licenses/by/4.0/>).